Inorg. Chem. **2008**, *47*, 7840−7851

Lanthanide Complexes Based on a 1,7-Diaza-12-crown-4 Platform Containing Picolinate Pendants: A New Structural Entry for the Design of Magnetic Resonance Imaging Contrast Agents

Marta Mato-Iglesias,[†] Adrián Roca-Sabio,[†] Zoltán Pálinkás,[‡] David Esteban-Gómez,[†] Carlos Platas-Iglesias,*[,†] Éva Tóth,[‡] Andrés de Blas,[†] and Teresa Rodríguez-Blas*[,†]

Departamento de Química Fundamental, Universidade da Coruña, Campus da Zapateira, Alejandro de la Sota 1, 15008 A Coruña, Spain, and Centre de Biophysique Moléculaire, CNRS, rue Charles Sadron, 45071 Orléans, Cedex 2, France

Received May 14, 2008

We have synthesized a new macrocyclic ligand, *N,N′*-Bis[(6-carboxy-2-pyridyl)methyl]-1,7-diaza-12-crown-4 (H_2bp12c4), designed for complexation of lanthanide ions in aqueous solution. The X-ray crystal structure of the Gd^{III} complex shows that the metal ion is directly bound to the eight donor atoms of the bp12c4 ligand, the ninth coordination site being occupied by an oxygen atom of a carboxylate group of a neighboring $[Gd(bp12c4)]^+$ unit, while the structure of the Lu^{III} analogue shows the metal ion being only eight-coordinate. The hydration numbers obtained from luminescence lifetime measurements in aqueous solution of the Eu^{III} and Tb^{III} complexes suggest an equilibrium in aqueous solution between a dihydrated ($q = 2$), ten-coordinate and a monohydrated ($q = 1$), nine-coordinate species. This has been confirmed by a variable temperature UV−vis spectrophotometric study on the Eu^{III} complex. The structure of the complexes in solution has been investigated by ^{1}H and ^{13}C NMR spectroscopy, as well as by theoretical calculations performed at the DFT (B3LYP) level. The results indicate that the change in hydration number occurring around the middle of the lanthanide series is accompanied by a change in the conformation adopted by the complexes in solution [$\Delta(\lambda\lambda\lambda\lambda)$ for $q = 2$ and $\Lambda(\delta\lambda\delta\lambda)$ for $q = 1$]. The structure calculated for the Yb^{III} complex ($\Lambda(\delta\lambda\delta\lambda)$) is in good agreement with the experimental structure in solution, as demonstrated by the analysis of the Yb^{III}-induced paramagnetic ^{1}H shifts.

Introduction

Lanthanide complexes of polydentate ligands containing picolinate pendants are of potential interest for application in time-resolved luminescence imaging[1] or as contrast agents in magnetic resonance imaging (MRI).[2] Recently we have reported a new series of octadentate acyclic ligands containing picolinate units and carboxylate[3] or phosphonate[4,5] pendants, and their Gd^{III} complexes have been shown to possess interesting relaxation properties. These ligands form stable nine-coordinate complexes with Ln^{III} ions in aqueous solution,[6,7] where a water molecule completes the inner coordination sphere. On the basis of structural considerations, we were able to control the water exchange rate of the inner sphere water molecule in the corresponding Gd^{III} complexes,

* To whom correspondence should be addressed. E-mail: cplatas@udc.es (C.P.-I.), mayter@udc.es (T.R.-B.).
[†] Universidade da Coruña.
[‡] Centre de Biophysique Moléculaire, CNRS.

(1) (a) Chatterton, N.; Bretonniere, Y.; Pecaut, J.; Mazzanti, M. *Angew. Chem., Int. Ed.* **2005**, *44*, 7595–7598. (b) Weibel, N.; Charbonnière, L.; Ziessel, R. *Tetrahedron Lett.* **2006**, *47*, 1793–1796.
(2) (a) Borel, A.; Kang, H.; Gateau, C.; Mazzanti, M.; Clarkson, R. B.; Belford, R. L. *J. Phys. Chem. A* **2006**, *110*, 1243412 438. (b) Fries, P. H.; Gateau, C.; Mazzanti, M. *J. Am. Chem. Soc.* **2005**, *127*, 15801–15814. (c) Gateau, C.; Mazzanti, M.; Pecaut, J.; Dunand, F. A.; Helm, L. *Dalton Trans.* **2003**, 2428–2433. (d) Bretonniere, Y.; Mazzanti, M.; Pecaut, J.; Dunand, F. A.; Merbach, A. E. *Chem. Commun.* **2001**, 621–622. (e) Bretonniere, Y.; Mazzanti, M.; Pecaut, J.; Dunand, F. A.; Merbach, A. E. *Inorg. Chem.* **2001**, *40*, 6737–6745. (f) Nonat, A.; Fries, P. H.; Pecaut, J.; Mazzanti, M. *Chem.—Eur. J.* **2007**, *13*, 8489–8506.
(3) Platas-Iglesias, C.; Mato-Iglesias, M.; Djanashvili, K.; Muller, R. N.; Vander Elst, L.; Peters, J. A.; de Blas, A.; Rodríguez-Blas, T. *Chem.—Eur. J.* **2004**, *10*, 3579–3590.
(4) Mato-Iglesias, M.; Platas-Iglesias, C.; Djanashvili, K.; Peters, J. A.; Tóth, É.; Balogh, E.; Muller, R. N.; Vander Elst, L.; de Blas, A.; Rodríguez-Blas, T. *Chem. Commun.* **2005**, 47294731.
(5) Balogh, E.; Mato-Iglesias, M.; Platas-Iglesias, C.; Tóth, É.; Djanashvili, K.; Peters, J. A.; de Blas, A.; Rodríguez-Blas, T. *Inorg. Chem.* **2006**, *45*, 8719–8728.
(6) Mato-Iglesias, M.; Balogh, E.; Platas-Iglesias, C.; Tóth, É.; de Blas, A.; Rodríguez-Blas, T. *Dalton Trans.* **2006**, *540*, 4–5415.
(7) Chatterton, N.; Gateau, C.; Mazzanti, M.; Pécaut, J.; Borel, A.; Helm, L.; Merbach, A. *Dalton Trans.* **2005**, 1129–1135.

10.1021/ic800878x CCC: $40.75
Published on Web 08/02/2008

Scheme 1

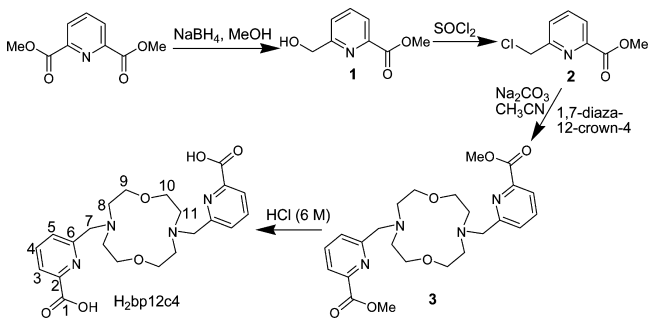

an important parameter to be optimized to obtain efficient MRI contrast agents. While numerous lanthanide complexes have been reported with acyclic ligands containing picolinate units,[1,3,8] examples with macrocyclic ligands bearing picolinate pendants are very scarce.[9]

Gd^{III} complexes to be used as MRI contrast agents must be stable enough to avoid the in vivo release of toxic free Gd^{III}. It has been demonstrated that, in addition to a high thermodynamic stability, kinetic factors must be taken into account to explain the in vivo behavior of Gd^{III} complexes. Indeed, a high thermodynamic stability of a Gd^{III} complex with a particular ligand does not necessarily prevent complex dissociation in vivo, even if a good selectivity for this metal ion over other endogeneous metal ions such as Ca^{II}, Zn^{II} or Cu^{II} is observed.[10] A correlation could be established between the long-term Gd^{III} deposition in the body and the rate of dissociation of a particular complex.[11] The issue of Gd^{III} toxicity is receiving much attention nowadays, since the recently described disease nephrogenic systemic fibrosis,[12] identified in patients with severe renal failure, has been associated with the use of Gd^{III} contrast agents based on DTPA-bisamide derivatives, which show relatively fast dissociation.[13] The dissociation kinetics of macrocyclic and linear lanthanide chelates differ substantially, the rigidity of macrocyclic chelates leading to considerably slower dissociation.[14]

In the search for innovative structural entries for the design of novel, kinetically inert MRI contrast agents, we report here the macrocyclic ligand *N,N′*-Bis[(6-carboxy-2-pyridyl)-methyl]-1,7-diaza-12-crown-4 (H_2bp12c4, Scheme 1). The most common coordination numbers observed in aqueous solution for Ln^{III} coordination compounds are 8 and 9. bp12c4 is a potentially octadentate ligand for lanthanide coordination, and thus it is expected to leave additional coordination position for at least one inner-sphere water molecule. The corresponding lanthanide complexes were characterized by ^{1}H and ^{13}C NMR techniques in D_2O solution. Luminescence lifetime measurements on the Eu^{III} and Tb^{III} complexes have been carried out to determine the hydration number of the complexes in solution. To further investigate a possible hydration equilibrium in aqueous solution, we have also performed a variable temperature high-resolution UV−vis spectrophotometric study on the Eu^{III} complex. In addition, the complexes were characterized by density functional theory (DFT) calculations carried out at the B3LYP level. The structure established by these calculations for the Yb^{III} complex was compared with the structural information obtained in solution from paramagnetic NMR measurements (Yb^{III}-induced ^{1}H NMR shifts).

Experimental Section

Physical Methods. Elemental analyses were carried out on a Carlo Erba 1108 elemental analyzer. FAB mass spectra were recorded using a FISONS QUATRO mass spectrometer with a Cs ion-gun and 3-nitrobenzyl alcohol as matrix. IR-spectra were recorded using a Bruker Vector 22 spectrophotometer equipped with a Golden Gate Attenuated Total Reflectance (ATR) accessory (Specac). UV−vis spectra were recorded on a Perkin-Elmer Lambda 900 spectrophotometer in 1.0 cm path quartz cells. High resolution UV−vis spectra on aqueous solutions of the Eu^{III} complex were recorded in the temperature range 15−60 °C on a Perkin-Elmer Lambda 19 spectrophotometer, in thermostatizable cells with a 10 cm optical length (577.0−581.0 nm). Excitation and emission spectra were recorded on a Perkin-Elmer LS-50B spectrometer equipped for low-temperature (77 K) measurements. Luminescence lifetimes were calculated from the monoexponential fitting of the average decay data, and they are averages of at least 3−5 independent determinations. ^{1}H and ^{13}C NMR spectra were recorded at 25 °C on Bruker Avance 300 and Bruker Avance 500 MHz spectrometers. For measurements in D_2O, *tert*-butyl alcohol was used as an internal standard with the methyl signal calibrated at $\delta = 1.2$ (^{1}H) and 31.2 ppm (^{13}C). Spectral assignments were based in part on two-dimensional COSY, HMQC, and HMBC experiments.

Chemicals and Starting Materials. Dimethylpyridine-2,6-dicarboxylate was prepared according to the literature method.[15] All other chemicals were purchased from commercial sources and used without further purification, unless otherwise stated. Silica gel (Fluka 60, 0.063−0.2 mm) was used for preparative column chromatography.

6-Hydroxymethylpyridine-2-carboxylic Acid Methyl Ester (1). $NaBH_4$ (4.310 g, 114.02 mmol) was added in small portions over a period of 0.5 h to a stirred solution of dimethylpyridine-2,6-dicarboxylate (7.445 g, 38.17 mmol) in MeOH (300 mL) at 0 °C. The mixture was stirred at 0 °C for 3 h and then a saturated $NaHCO_3$ aqueous solution (200 mL) was added. The MeOH was removed in a rotary evaporator and the resulting aqueous solution was extracted with $CHCl_3$ (5 × 100 mL). The combined organic extracts were dried over $MgSO_4$ and evaporated to give 4.370 g of **1** (69%) as a white solid. Anal. Calcd for $C_8H_9NO_3$: C, 57.5; H, 5.4; N, 8.4%. Found: C, 56.9; H, 5.3; N, 8.3%. δ_H (solvent $CDCl_3$,

(8) (a) Charbonnière, L.; Weibel, N.; Retailleau, P.; Ziessel, R. *Chem.−Eur. J.* **2007**, *13*, 346–358. (b) Charbonnière, L.; Mameri, S.; Kadjane, P.; Platas-Iglesias, C.; Ziessel, R. *Inorg. Chem.* **2008**, *47*, 3748–3762.
(9) Nonat, A.; Gateau, C.; Fries, P. H.; Mazzanti, M. *Chem.−Eur. J.* **2006**, *12*, 7133–7150.
(10) Brücher, E.; Sherry, A. D. Stability and Toxicity of Contrast Agents. In *The Chemistry of Contrast Agents in Medical Magnetic Resonante Imaging*; Tóth, E., Merbach, A. E., Eds.; Wiley: Chichester, 2001; pp. 243−279.
(11) Wedeking, P.; Kumar, K.; Tweedle, M. F. *Magn. Reson. Imaging* **1992**, *10*, 641–648.
(12) Cheng, S.; Abramova, L.; Saab, G.; Turabelidze, G.; Patel, P.; Arduino, M.; Hess, T.; Kallen, A.; Jhung, M. *JAMA* **2007**, *297*, 1542–1544.
(13) Sarka, L.; Burai, L.; Kiraly, R.; Zekany, L.; Brücher, E. *J. Inorg. Biochem.* **2002**, *91*, 320–326.
(14) Brücher, E. *Top. Curr. Chem.* **2002**, *221*, 103–122.
(15) Chrystal, E. J. T.; Couper, L.; Robins, D. J. *Tetrahedron* **1995**, *51*, 10241–10252.

295 K, 300 MHz): 8.02 (d, 1H, py, $^3J = 7.7$ Hz); 7.84 (t, 1H, py); 7.54 (d, 1H, py, $^3J = 7.8$ Hz); 4.86 (s, 2H, -CH_2-); 3.99 (s, 3H, -OCH_3). δ_C (solvent $CDCl_3$, 295 K, 75.5 MHz): 52.6 (primary C); 64.6 (secondary C); 137.7, 124.0, 123.8 (tertiary C); 165.5, 160.3, 146.9 (quaternary C). IR: 1740 ν(C═O), 1591 $\nu(C{=}N)_{py}$ cm^{-1}. FAB-MS (*m*/*z*(%BPI)): 168 (100) $[\mathbf{1} + H]^+$.

6-Chloromethylpyridine-2-carboxylic Acid Methyl Ester (2). $SOCl_2$ (5 mL) was added over **1** (1.20 g, 7.18 mmol) at 0 °C under an inert atmosphere (Ar). The mixture was stirred at 0 °C for 1 h, and the excess of $SOCl_2$ was removed under reduced pressure. The residue was dissolved in toluene (50 mL), and the organic solution, washed with a 1 M $NaHCO_3$ aqueous solution. The organic extract was evaporated, and the resulting oily residue was precipitated by addition of diethyl ether to give 1.09 g of **2** (82%) as a pale yellow solid. Anal. Calcd for $C_8H_8ClNO_2$: C, 51.8; H, 4.3; N, 7.6%. Found: C, 51.6; H, 4.4; N, 7.6%. δ_H (solvent $CDCl_3$, 295 K, 300 MHz): 8.09 (d, 1H, py, $^3J = 7.6$ Hz); 7.90 (t, 1H, py); 7.75 (d, 1H, py, $^3J = 7.6$ Hz); 4.79 (s, 2H, -CH_2-); 4.02 (s, 3H, -OCH_3). δ_C (solvent $CDCl_3$, 295 K, 75.5 MHz): 43.0 (primary C); 46.2 (secondary C); 138.1, 126.1, 124.4 (tertiary C); 165.3, 157.2, 147.4 (quaternary C). IR: 1738 ν(C═O), 1581 $\nu(C{=}N)_{py}$ cm^{-1}. FAB-MS (*m*/*z*(%BPI)): 186(100) $[\mathbf{2} + H]^+$.

***N,N′*-Bis[(6-methoxycarbonyl-2-pyridyl)methyl]-1,7-diaza-12-crown-4 (3).** Compound **2** (2.000 g, 10.78 mmol) and Na_2CO_3 (3.400 g, 32.08 mmol) were added to a solution of 1,7-diaza-12-crown-4 (0.946 g, 5.43 mmol) in acetonitrile (75 mL). The mixture was heated to reflux with stirring for a period of 24 h, and then the excess of Na_2CO_3 was filtered off. The filtrate was concentrated to dryness, and the yellow residue partitioned between equal volumes (200 mL) of H_2O and CH_2Cl_2. The organic phase was separated, dried over $MgSO_4$, filtered, and evaporated to dryness. Addition of hexane gave 1.922 g of **3** (75%) as a pale yellow solid. Anal. Calcd for $C_{24}H_{32}N_4O_6$: C, 61.0; H, 6.8; N, 11.8%. Found: C, 60.4; H, 6.7; N, 11.5%. δ_H (solvent $CDCl_3$, 295 K, 300 MHz): 8.09 (d, 2H, py, $^3J = 8.6$ Hz); 8.01 (d, 2H, py,$^3J = 7.6$ Hz); 7.82 (t, 2H, py); 4.00 (s, 6H, -OCH_3); 3.97 (s, 4H, -CH_2-); 3.63 (t,$^3J = 4.6$ Hz 8H, -CH_2-); 2.83 (m, 8H, -CH_2-). δ_C (solvent $CDCl_3$, 295 K, 75.5 MHz): 52.9 (primary C); 55.3, 62.2, 69.5 (secondary C); 123.5, 126.3, 137.3 (tertiary C); 147.1, 161.4, 165.9 (quaternary C). IR: 1709 ν(C═O), 1589 $\nu(C{=}N)_{py}$ cm^{-1}. FAB-MS (*m*/*z*(%BPI)): 473(100) $[\mathbf{3} + H]^+$.

***N,N′*-Bis[(6-carboxy-2-pyridyl)methyl]-1,7-diaza-12-crown-4 (H_2bp12c4·4HCl).** A solution of compound **3** (1.000 g, 2.12 mmol) in 6 M HCl (10 mL) was heated to reflux for 12 h. After cooling to room temperature the white solid formed was collected by filtration to give 1.044 g (81%) of the desired compound. Anal. Calcd for $C_{22}H_{28}N_4O_6 \cdot 4HCl \cdot H_2O$: C, 43.4; H, 5.6; N, 9.2%. Found: C, 43.4; H, 6.4; N, 9.1%. δ_H (solvent D_2O, 295 K, 300 MHz, pD = 8.0): 7.98 (t, 2H, py); 7.89 (d, 2H, py, $^3J = 7.7$ Hz); 7.65 (d, 2H, py, $^3J = 7.6$ Hz); 4.07 (s, 4H, -CH_2-); 3.55 (t, $^3J = 4.6$ Hz, 8H, -CH_2-); 3.02 (t, $^3J = 4.6$ Hz, 8H, -CH_2-). δ_C (solvent D_2O, 295 K, 75.5 MHz, pD = 8.0): 55.4, 62.8, 68.3 (secondary C); 140.3, 128.7, 124.9 (tertiary C); 174.6, 156.1, 155.1 (quaternary C). IR: 1697 ν(C═O), 1592 $\nu(C{=}N)_{py}$ cm^{-1}. FAB-MS (*m*/*z*(%BPI)): 445(100) $[H_3bp12c4]^+$.

Analysis of the LIS data. Lanthanide induced paramagnetic shifts (LIS) of $[Yb(bp12c4)(H_2O)]^+$ complex were calculated using the corresponding Lu^{III} complex as diamagnetic reference. The LIS values were analyzed with the "SHIFT ANALYSIS" program developed by Forsberg,[16] where no assumption is made about the magnetic symmetry of the complex. The in vacuo and in aqueous solution B3LYP optimized structures of this complex in $\Lambda(\lambda\lambda\lambda\lambda)$, $\Delta(\lambda\lambda\lambda\lambda)$, and $\Lambda(\delta\lambda\delta\lambda)$ conformations were used as input geometries. The agreement factors between the observed and calculated values were determined according to eq 1:[17]

$$AF_i = \left[\sum_j (\delta_{ij}^{exp} - \delta_{ij}^{cal})^2 / \sum_j (\delta_{ij}^{exp})^2\right]^{1/2} \quad (1)$$

where δ_{ij}^{exp} and δ_{ij}^{cal} represent the experimental and calculated values of a nucleus *i* in a given Ln^{III} complex *j*, respectively.

Computational Methods. All calculations were performed employing hybrid DFT with the B3LYP exchange-correlation functional,[18,19] and the Gaussian 03 package (Revision C.01).[20] Full geometry optimizations of the $[Ln(bp12c4)(H_2O)]^+$ and $[Ln(bp12c4)(H_2O)_2]^+$ (Ln = La, Nd, Gd, Ho, Yb or Lu) systems were performed in vacuo by using the effective core potential (ECP) of Dolg et al. and the related [5s4p3d]-GTO valence basis set for the lanthanides,[21] and the 6−31G(d) basis set for C, H, N, and O atoms. The stationary points found on the potential energy surfaces as a result of the geometry optimizations have been tested to represent energy minima rather than saddle points via frequency analysis.

In aqueous solution relative free energies of the $\Lambda(\lambda\lambda\lambda\lambda)$, $\Delta(\lambda\lambda\lambda\lambda)$, and $\Lambda(\delta\lambda\delta\lambda)$ isomers were calculated from solvated single point energy calculations on the geometries optimized in vacuo. In these calculations the 6−31G(d) basis set was used for C, H, N, and O atoms. Solvent effects were evaluated by using the polarizable continuum model (PCM). In particular, we used the C-PCM variant[22] that employs conductor rather than dielectric boundary conditions. The solute cavity is built as an envelope of spheres centered on atoms or atomic groups with appropriate radii. Calculations were performed using an average area of 0.2 $Å^2$ for all the finite elements (tesserae) used to build the solute cavities. For lanthanides the previously parametrized radii were used.[23] Free energies include both electrostatic and nonelectrostatic contributions.

X-ray Crystal Structure Determinations. Three dimensional X-ray data were collected on a Bruker X8 APEXII CCD for compound **4** and on a Bruker Smart 1000 CCD for **5.** Data were corrected for Lorentz and polarization effects and for absorption

(16) Forsberg, J. H.; Delaney, R. M.; Zhao, Q.; Harakas, G.; Chandran, R. *Inorg. Chem.* **1995**, *34*, 3705–3715.

(17) Davis, R. E.; Willcott, M. R. *J. Am. Chem. Soc.* **1972**, *94*, 1744–1745.

(18) Becke, A. D. *J. Chem. Phys.* **1993**, *98*, 5648–5652.

(19) Lee, C.; Yang, W.; Parr, R. G. *Phys. Rev. B* **1988**, *37*, 785–789.

(20) Frisch, M. J. ; Trucks, G. W.; Schlegel, H. B.; Scuseria, G. E.; Robb, M. A.; Cheeseman, J. R.; Montgomery, Jr., J. A.; Vreven, T.; Kudin, K. N.; Burant, J. C.; Millam, J. M.; Iyengar, S. S.; Tomasi, J.; Barone, V.; Mennucci, B.; Cossi, M.; Scalmani, G.; Rega, N.; Petersson, G. A.; Nakatsuji, H.; Hada, M.; Ehara, M.; Toyota, K.; Fukuda, R.; Hasegawa, J.; Ishida, M.; Nakajima, T.; Honda, Y.; Kitao, O.; Nakai, H.; Klene, M.; Li, X.; Knox, J. E.; Hratchian, H. P.; Cross, J. B.; Adamo, C.; Jaramillo, J.; Gomperts, R.; Stratmann, R. E.; Yazyev, O.; Austin, A. J.; Cammi, R.; Pomelli, C.; Ochterski, J. W.; Ayala, P. Y.; Morokuma, K.; Voth, G. A.; Salvador, P.; Dannenberg, J. J.; Zakrzewski, V. G.; Dapprich, S.; Daniels, A. D.; Strain, M. C.; Farkas, O.; Malick, D. K.; Rabuck, A. D.; Raghavachari, K.; Foresman, J. B.; Ortiz, J. V.; Cui, Q.; Baboul, A. G.; Clifford, S.; Cioslowski, J.; Stefanov, B. B.; Liu, G.; Liashenko, A.; Piskorz, P.; Komaromi, I.; Martin, R. L.; Fox, D. J.; Keith, T.; Al-Laham, M. A.; Peng, C. Y.; Nanayakkara, A.; Challacombe, M.; Gill, P. M. W.; Johnson, B.; Chen, W.; Wong, M. W.; Gonzalez, C.; Pople, J. A. *Gaussian 03*, Revision C.01; Gaussian, Inc.: Wallingford CT, 2004.

(21) Dolg, M.; Stoll, H.; Savin, A.; Preuss, H. *Theor. Chim. Acta* **1989**, *75*, 173–194.

(22) Barone, V.; Cossi, M. *J. Phys. Chem. A* **1998**, *102*, 1995–2001.

(23) Cosentino, U.; Villa, A.; Pitea, D.; Moro, G.; Barone, V. *J. Phys. Chem. B* **2000**, *104*, 8001–8007.

Table 1. Crystal Data and Structure Refinement for **4** and **5**

	[Gd(bp12c4)]Cl·MeOH	[Lu(bp12c4)]Cl·MeOH·3H$_2$O
formula	$C_{23}H_{30}ClGdN_4O_7$	$C_{23}H_{36}ClLuN_4O_{10}$
MW	667.21	738.98
space group	$P2_1/n$	$P\bar{1}$
crystal system	monoclinic	triclinic
a/Å	11.1596(6)	8.642(2)
b/Å	11.5025(7)	8.793(2)
c/Å	23.346(1)	18.355(4)
α/deg	90	99.883(4)
β/deg	102.754(1)	91.113(4)
γ/deg	90	98.435(4)
V/Å^3	2922.9(3)	1357.7(5)
Z	4	2
T/K	100.0(2)	100.0(2)
λ, Å (Mo Kα)	0.71073	0.71073
D_{calc}/g cm^{-3}	1.516	1.808
μ/mm^{-1}	2.404	3.796
R_{int}	0.0193	0.0657
reflns measd	7145	6723
reflns obsd	6741	5436
R_1[a]	0.0377	0.0388
wR_2 (all data)[b]	0.1179	0.0747

[a] $R_1 = \sum||F_o| - |F_c||/\sum|F_o|$. [b] $wR_2 = \{\sum[w(|F_o|^2 - |F_c|^2)^2]/\sum[w(F_o^4)]\}^{1/2}$.

by semiempirical methods[24] based on symmetry-equivalent reflections. Complex scattering factors were taken from the program SHELX97[25] included in the WinGX program system[26] as implemented on a Pentium computer. Both structures were solved by Patterson methods (DIRDIF99)[27] and refined[25] by full-matrix least-squares on F^2. For **4** all hydrogen atoms were included in calculated positions and refined in riding mode. For **5** the hydrogen atoms were also included in calculated positions and refined in riding mode except for the hydrogen atoms of the water molecules, which were first located in a difference electron-density map, and the distance fixed to the corresponding oxygen atom. For **5** refinement converged with anisotropic displacement parameters for all non-hydrogen atoms, while for **4** there were some problems of convergence with heavily disordered solvent molecules, so that it was necessary to clean up those areas with the program SQUEEZE implemented in the PLATON[28] program system, and finally refinement converged with anisotropic displacement parameters for all non-hydrogen atoms as well. Both crystals present disorders in the chloride anion that have been resolved with occupancy factors of 0.4(1) and 0.47(2) for Cl(1) in **4** and **5**, respectively. In the crystal of the Lu complex a methanol molecule and a water molecule were also disordered. This disorders have been solved with occupancy factors of 0.60(9) for O(10A) and C(23A) and 0.50(1) for O(9). Crystal data and details on data collection and refinement are summarized in Table 1.

Results and Discussion

Synthesis of the Ligand. Ligand H$_2$bp12c4 (Scheme 1) was obtained in four steps from dimethylpyridine-2,6-dicarboxylate with an overall yield of 34% using the procedure described in the Experimental Section (Scheme 1). The 6-chloromethylpyridine derivative **2** was prepared in good yield by partial reduction of dimethylpyridine-2,6-dicarboxylate followed by reaction of the intermediate alcohol **1** with $SOCl_2$. Alkylation of 1,7-diaza-12-crown-4 with **2** in refluxing acetonitrile in the presence of Na_2CO_3 gave compound **3** in 75% yield. Full deprotection of the methyl esters of **3** was cleanly achieved with 6 M HCl to yield the desired ligand H$_2$bp12c4.

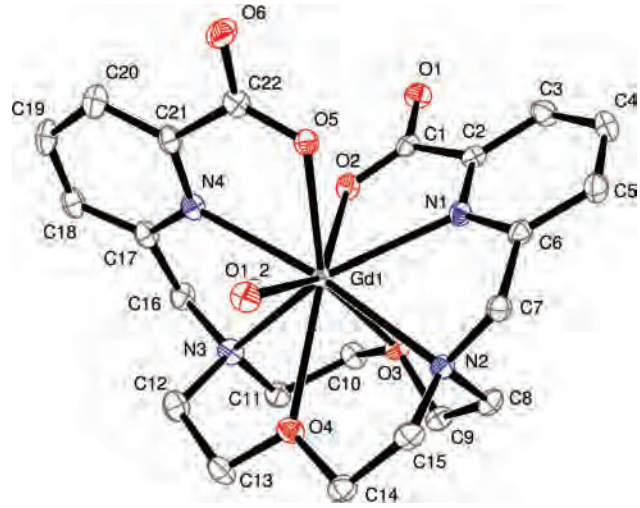

Figure 1. X-ray crystal structure of the cation [Gd(bp12c4)]$^+$ in **4** with atom labeling; hydrogen atoms are omitted for simplicity. The ORTEP plots are drawn at the 50% probability level.

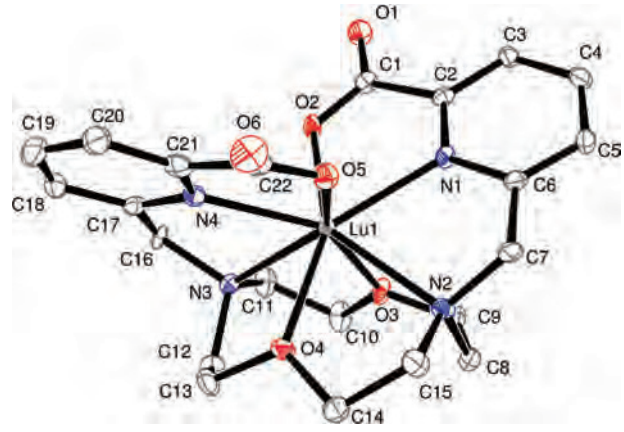

Figure 2. X-ray crystal structure of the cation [Lu(bp12c4)]$^+$ in **5** with atom labeling; hydrogen atoms are omitted for simplicity. The ORTEP plots are drawn at the 50% probability level.

X-ray Crystal Structures. The solid state structures of compounds **4** and **5** have been determined by X-ray diffraction studies. Crystals were obtained by slow evaporation of solutions of the complexes prepared in situ in 2-propanol. Attempts to obtain single crystals of the complexes from aqueous solutions were unsuccessful. Crystals contain the cations [Ln(bp12c4)]$^+$ (**4**, Ln = Gd; **5**, Ln = Lu), one chloride anion and methanol and/or water molecules. Figures 1 and 2 show a view of the complex cations, while bond distances and angles of the metal coordination environment are given in Table 2. In [Gd(bp12c4)]$^+$ the metal ion is directly bound to the eight donor atoms of the bp12c4 ligand,

(24) Sheldrick, G. M. *SADABS*, Version 2.10; University of Göttingen: Germany, 2004.
(25) G. M. Sheldrick *SHELX97 [Includes SHELXS97, SHELXL97, CIFTAB] - Programs for Crystal Structure Analysis Release 97−2*; Institüt für Anorganische Chemie der Universität Göttingen: Göttingen, Germany, 1998.
(26) Farrugia, L. J. *WinGX MS-Windows system of programs for solving, refining and analysing single crystal X-ray diffraction data for small molecules, J. Appl. Cryst.* **1999**, *32*, 837–838.
(27) Beurskens, P. T.; Beurskens, G.; de Gelder, R.; Garcia-Granda, S.; Gould, R. O.; Israel, R.; Smits, J. M. M. *DIRDIF99 program system*; Crystallography Laboratory, University of Nijmegen: The Netherlands, 1999.
(28) Spek, A. L. *PLATON, A Multipurpose Crystallographic Tool*; Utrecht University: Utrecht, The Netherlands, 2007.

Table 2. Selected Bond Lengths (Å) and Angles (deg) for $[Ln(bp12c4)]^+$ Complexes (Ln = Gd or Lu) in Compounds **4** and **5**[a]

	4		5
Gd(1)−O(2)	2.404(3)	Lu(1)−O(5)	2.208(3)
Gd(1)−O(4)	2.565(3)	Lu(1)−O(2)	2.218(3)
Gd(1)−O(3)	2.449(3)	Lu(1)−O(3)	2.303(3)
Gd(1)−O(5)	2.372(3)	Lu(1)−O(4)	2.319(3)
Gd(1)−N(3)	2.617(4)	Lu(1)−N(1)	2.347(4)
Gd(1)−N(2)	2.617(4)	Lu(1)−N(4)	2.359(4)
Gd(1)−N(4)	2.493(4)	Lu(1)−N(2)	2.481(4)
Gd(1)−N(1)	2.494(4)	Lu(1)−N(3)	2.486(4)
Gd(1)−O(1)	2.351(3)		
O(1)−Gd(1)−O(5)	72.37(12)	O(5)−Lu(1)−O(2)	105.21(12)
O(1)−Gd(1)−O(2)	144.31(12)	O(5)−Lu(1)−O(3)	153.21(11)
O(5)−Gd(1)−O(2)	75.84(11)	O(2)−Lu(1)−O(3)	89.20(12)
O(1)−Gd(1)−O(3)	142.06(11)	O(5)−Lu(1)−O(4)	85.94(12)
O(5)−Gd(1)−O(3)	142.57(11)	O(2)−Lu(1)−O(4)	152.84(11)
O(2)−Gd(1)−O(3)	73.34(11)	O(3)−Lu(1)−O(4)	91.27(12)
O(1)−Gd(1)−N(4)	79.28(12)	O(5)−Lu(1)−N(1)	84.05(13)
O(5)−Gd(1)−N(4)	65.28(12)	O(2)−Lu(1)−N(1)	69.24(12)
O(2)−Gd(1)−N(4)	72.96(12)	O(3)−Lu(1)−N(1)	80.10(12)
O(3)−Gd(1)−N(4)	123.09(12)	O(4)−Lu(1)−N(1)	137.47(12)
O(1)−Gd(1)- N(1)	118.61(12)	O(5)−Lu(1)−N(4)	69.41(13)
O(5)−Gd(1)−N(1)	73.16(12)	O(2)−Lu(1)−N(4)	83.27(12)
O(2)−Gd(1)−N(1)	65.30(12)	O(3)−Lu(1)−N(4)	135.84(12)
O(3)−Gd(1)−N(1)	74.97(12)	O(4)−Lu(1)−N(4)	77.56(12)
N(4)−Gd(1)−N(1)	126.56(13)	N(1)−Lu(1)−N(4)	135.14(13)
O(1)−Gd(1)−O(4)	66.90(12)	O(5)−Lu(1)−N(2)	83.14(12)
O(5)−Gd(1)−O(4)	139.13(11)	O(3)−Lu(1)−N(2)	71.07(12)
O(2)−Gd(1)−O(4)	143.70(11)	O(4)−Lu(1)−N(2)	68.90(12)
O(3)−Gd(1)−O(4)	76.36(11)	N(1)−Lu(1)−N(2)	68.90(13)
N(4)−Gd(1)−O(4)	108.86(12)	N(4)−Lu(1)−N(2)	137.85(13)
N(1)−Gd(1)−O(4)	124.56(12)	O(5)−Lu(1)−N(3)	134.57(13)
O(1)−Gd(1)−N(2)	86.27(12)	O(2)−Lu(1)−N(3)	83.29(12)
O(5)−Gd(1)−N(2)	112.45(12)	O(3)−Lu(1)−N(3)	68.48(12)
O(2)−Gd(1)−N(2)	121.20(11)	O(4)−Lu(1)−N(3)	71.70(12)
O(3)−Gd(1)−N(2)	68.16(11)	N(1)−Lu(1)−N(3)	138.36(13)
N(4)−Gd(1)−N(2)	165.37(13)	N(4)−Lu(1)−N(3)	67.44(13)
N(1)−Gd(1)−N(2)	62.93(12)	N(2)−Lu(1)−N(3)	121.56(12)
O(4)−Gd(1)−N(2)	62.60(11)		
O(1)−Gd(1)−N(3)	100.80(12)		
O(5)−Gd(1)−N(3)	130.47(12)		
O(2)−Gd(1)−N(3)	87.66(12)		
O(3)−Gd(1)−N(3)	68.88(12)		
N(4)−Gd(1)−N(3)	65.26(13)		
N(1)−Gd(1)−N(3)	139.85(12)		
O(4)−Gd(1)−N(3)	62.79(12)		
N(2)−Gd(1)−N(3)	115.99(12)		

[a] See Figures 1 and 2 for labeling.

nine-coordination being completed by an oxygen atom of a carboxylate group of a neighboring $[Gd(bp12c4)]^+$ unit. This results in the formation of a one-dimensional coordination polymer by sharing carboxylic groups between adjacent chelates, as previously observed for the Gd^{III} complex of 1-oxa-4,7,10-triazaciclododecane-4,7,10-triacetic acid (odotra).[29] In contrast, in the $[Lu(bp12c4)]^+$ cation the Lu^{III} ion is only bound to the eight available donor atoms of the ligand. Thus, the solid state structures of the Gd^{III} and Lu^{III} complexes of bp12c4 evidence a decrease of the coordination number of the metal ion from nine to eight as the ionic radius of the Ln^{III} ion decreases. Changes in the coordination number along the lanthanide series are often observed for Ln^{III} complexes both in the solid state and in solution.[30] The distances between the Ln^{III} ion and the oxygen atoms of the crown moiety are shorter than those between the metal ion and the pivotal nitrogen atoms, as previously observed in Ln^{III} complexes derived from 1,7-diaza-12-crown-4.[31] The distances between the lanthanide and the donor atoms of the picolinate pendants are about 0.04−0.09 Å shorter than those found for nine-coordinate Gd^{III} and eight-coordinate Lu^{III} complexes of acyclic ligands containing picolinate moieties.[32]

In both complexes, the side arms of the ligand are placed above the plane of the macrocyclic unit, resulting in a *syn* conformation. Likewise, the lone pairs of both pivotal nitrogen atoms are directed inward to the receptor cavity in an *endo-endo* arrangement. The $[Lu(bp12c4)]^+$ cation shows a slightly distorted C_2 symmetry in the solid state, where the symmetry axis is perpendicular to the pseudoplane described by the four donor atoms of the crown moiety and contains the Lu^{III} ion. In $[Gd(bp12c4)]^+$, the coordination of the oxygen atom of the neighboring cation [O(1), see Figure 1] results in an angle of 100.7° between the vectors O(1)−Gd(1) and Gd(1)−Z, where Z is the centroid described by the four donor atoms of the crown moiety. Moreover, the donor atom O(1) is situated between the picolinate unit containing O(5) and the fragment of the crown moiety containing O(4) and not between the two picolinate units. As a consequence, the $[Gd(bp12c4)]^+$ shows a C_1 symmetry in the solid state.

The coordination polyhedron around the Lu^{III} ion in **5** can be described as a severely distorted square antiprism composed of two parallel pseudo planes: N(1), N(4), O(2), and O(5) define the upper pseudo plane (mean deviation from planarity 0.223 Å), while N(2), N(3), O(3), and O(4) define the lower pseudo plane (mean deviation from planarity 0.202 Å). The angle between these two least-squares planes amounts to 1.5°, and the Lu^{III} ion is placed at 1.12 Å from the upper plane and 1.41 Å from the plane formed by N(2), N(3), O(3), and O(4). The mean twist angle, ω,[33] between these nearly parallel squares is 40.4°, which is a value that is very close to that expected for a square antiprism (ideal value 45°). The coordination polyhedron around the metal ion in $[Gd(bp12c4)]^+$ can be described either as a severely distorted tricapped trigonal prism or as a capped dodecahedron; an unambiguous assignment to one of these reference polyhedra is not possible.

The *syn* conformation of the ligand in the $[Ln(bp12c4)]^+$ complexes (Ln = Gd or Lu) implies the occurrence of two helicities (one belonging to the crown moiety and one associated with the layout of the pendant arms).[34,35] Inspection of the crystal structure data reveals that in the Lu^{III} complex two $\Delta(\lambda\lambda\lambda\lambda)$ and $\Lambda(\delta\delta\delta\delta)$ enantiomers co-crystallize in equal amounts (racemate). In the case of the Gd^{III}

(29) Spirlet, M.-R.; Rebizant, J.; Wang, X.; Jin, T.; Gilsoul, D.; Comblin, V.; Maton, F.; Muller, R. N.; Desreux, J. F. *J. Chem. Soc., Dalton Trans.* **1997**, 497–500.
(30) Valencia, L.; Martínez, J.; Macías, A.; Bastida, R.; Carvalho, R. A.; Geraldes, C. F. G. C. *Inorg. Chem.* **2002**, *41*, 5300–5312.
(31) Gonzalez Lorenzo, M.; De Blas, A.; Esteban Gomez, D.; Platas Iglesias, C.; Rodriguez-Blas, T. *Acta Crystallogr., Sect. C* **2006**, *C62*, m360−m362.
(32) Bretonnière, Y.; Mazzanti, M.; Pècaut, J.; Dunand, F. A.; Merbach, A. E. *Inorg. Chem.* **2001**, *40*, 6737–6745.
(33) Piguet, C.; Bünzli, J.-C. G.; Bernardinelli, G.; Bochet, C. G.; Froidevaux, P. *J. Chem. Soc., Dalton Trans.* **1995**, 83–97.
(34) Corey, E. J.; Bailar, J. C., Jr. *J. Am. Chem. Soc.* **1959**, *81*, 2620–2629.
(35) Beattie, J. K. *Acc. Chem. Res.* **1971**, *4*, 253–259.

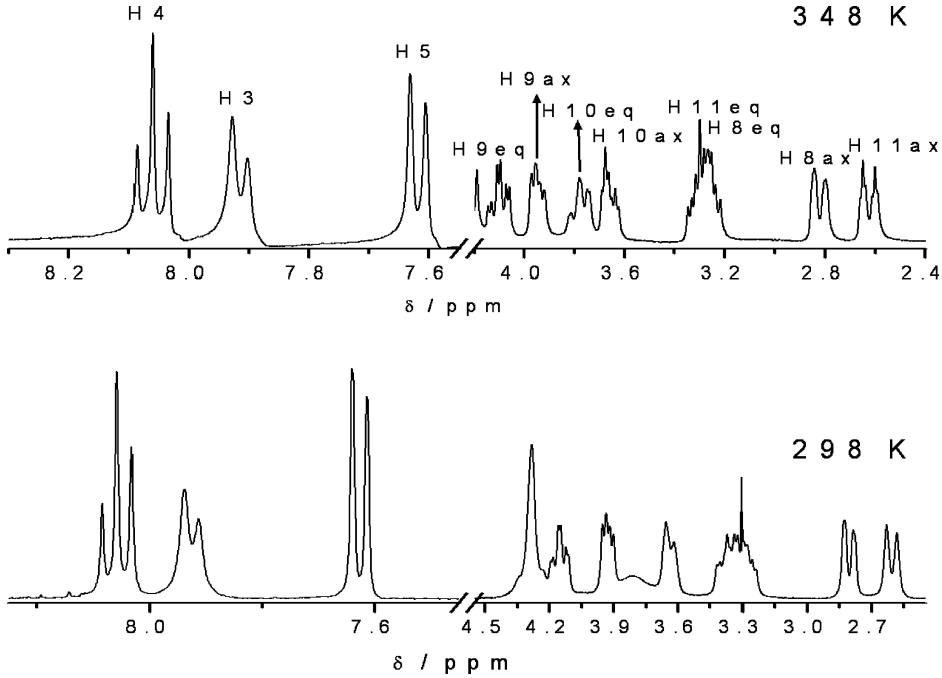

Figure 3. ^{1}H NMR spectra of the La^{III} complex of bp12c4 recorded in D_2O solution (pD = 7.0) at 298 K (bottom) and 348 K (top). See Scheme 1 for labeling.

analogue, two centrosymmetrically related enantiomers are also found in the crystal lattice: $\Lambda(\lambda\lambda\lambda\delta)$ and $\Delta(\delta\delta\delta\lambda)$.

^{1}H and ^{13}C NMR Spectra of the Diamagnetic Complexes. The ^{1}H and ^{13}C NMR spectra of the diamagnetic La^{III} and Lu^{III} complexes of bp12c4 were obtained in D_2O solution at pD = 7.0. While for the Lu^{III} complex the spectra are well-resolved at 298 K, in the case of the La^{III} analogue the ^{1}H NMR spectrum recorded at room temperature shows relatively broad signals for protons H7 and H10eq. Increasing the temperature to 348 K results in an appreciable sharpening of these signals, and a well-resolved spectrum of the complex could be obtained (Figure 3). The proton spectra of both complexes consist of 13 signals corresponding to 13 magnetically nonequivalent proton environments in the ligand (see Scheme 1 for labeling). This points to an effective C_2 symmetry of the complexes in solution. This is also confirmed by the ^{13}C NMR spectra, which show 11 peaks for the 22 carbon nuclei of the ligand backbone. The assignments of the proton signals (Table 3) were based upon HMQC and HMBC 2D heteronuclear experiments as well as standard 2D homonuclear COSY experiments, which gave strong cross-peaks between the geminal CH_2 protons (7−11) and between the ortho-coupled pyridyl protons. Although the specific CH_2 proton assignments of the axial and equatorial H7−H11 protons were not possible on the basis of the 2D NMR spectra, they were carried out using the stereochemically dependent proton shift effects, resulting from the polarization of the C−H bonds by the electric field effect caused by the cation charge.[36] This results in a deshielding of the equatorial protons which are pointing away from the Ln^{III} ion. The signals due to protons H7a and H7b show an AB pattern where the larger shift for H7b results from the combined deshielding effects of the pyridyl ring current and the polarizing effect of the Ln^{III} ion on the C−H bond pointing away from it. A specific assignment of several pairs of NMR signals (8−11, 9−10) was achieved with two-dimensional NOESY spectra, which show strong cross-peaks relating H7a and H11ax. The optimized DFT geometries described below predict H7a···H11ax distances of 2.1−2.2 Å. No evidence for interconversion between axial and equatorial protons is observed in the NMR spectra of the La^{III} and Lu^{III} complexes even at 348 K, which indicates an important conformational rigidity of these complexes in solution.

Table 3. ^{1}H and ^{13}C NMR Shifts[a] for La^{III} and Lu^{III} complexes of bp12c4[b]

^{1}H	La^{III}[c]	Lu^{III}[d]	^{13}C	La^{III}[c]	Lu^{III}[d]
H3	7.91(d)	8.03(d)	C1	*e*	174.3
H4	8.06(t)	8.24(t)	C2	153.3	155.1
H5	7.62(d)	7.83(d)	C3	125.5	125.5
H7a	4.24(d)	4.43(d)	C4	142.6	144.8
H7b	4.33(d)	4.77(d)	C5	127.2	127.4
H8ax	2.83	3.18	C6	158.8	159.6
H8eq	3.28	3.54	C7	64.1	65.2
H9ax	3.96	3.39	C8	54.6	56.5
H9eq	4.11	3.79	C9	71.0	72.1
H10ax	3.69	4.18	C10	71.3	73.2
H10eq	3.80	4.34	C11	54.3	56.0
H11ax	2.62	2.91			
H11eq	3.31	3.60			

[a] ppm with respect to TMS. [b] see Scheme 1 for labeling. [c] Assignment supported by 2D COSY, NOESY, HMQC, and HMBC experiments at 348 K; $^{3}J_{3,4}$ = 7.6 Hz; $^{3}J_{4,5}$ = 7.7 Hz; $^{2}J_{7a,7b}$ = 15.8 Hz. [d] Assignment supported by 2D COSY, NOESY, HMQC, and HMBC experiments at 298 K; $^{3}J_{3,4}$ = 7.5 Hz; $^{3}J_{4,5}$ = 7.8 Hz; $^{2}J_{7a,7b}$ = 16.5 Hz. [e] Not observed.

Assessment of the Hydration State. Luminescence lifetime measurements have been widely used for quantifying the number of inner sphere water molecules in lanthanide

(36) Harris, R. K. *Nuclear Magnetic Resonance Spectroscopy: A Physicochemical view*; Pitman: London, 1983.

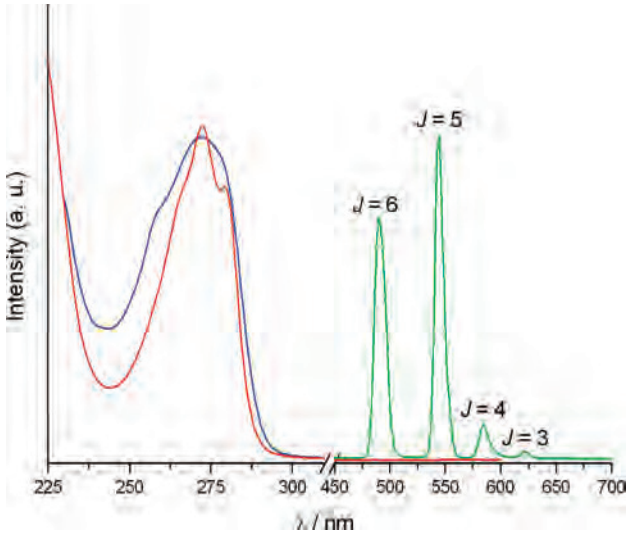

Figure 4. Absorption (red), excitation (blue), and emission (green) spectra of the Tb^{III} complex of bp12c4 as recorded in H_2O solution (10^{-5} M, pH = 8.9) at room temperature.

complexes.[37] Although ions that emit in the near-infrared such as Yb^{III} have also been used for this purpose,[38] Tb^{III} and Eu^{III} are most commonly applied for lifetime measurements because they emit in the visible region and show longer emission lifetimes. These two ions flank Gd^{III} in the periodic table; hence, they have nearly the same ratio of charge to ionic radius as Gd^{III} and correspondingly similar coordination chemistry. Therefore, the number of inner sphere water molecules determined for Tb^{III} and Eu^{III} complexes should be close to the value for Gd^{III} complexes. Moreover, a desirable optical property of the Ln^{III} complexes of bp12c4 is that the picolinate moieties can act as an antenna to sensitize the emission of Eu^{III} and Tb^{III}, which greatly increases the effective extinction coefficient of the metal ion excitation and therefore improve the sensitivity of the luminescence detection. Indeed, the absorption spectra of the Eu^{III} and Tb^{III} complexes show a band with a maximum at 272 nm and shoulders at 265 and 279 nm that can be assigned to a combination of $\pi \rightarrow \pi^*$ and $n \rightarrow \pi^*$ transitions centered on the picolinate moieties (Figure 4).[39]

The emission spectra of about 10^{-5} M solutions of the Eu^{III} and Tb^{III} complexes of bp12c4 in H_2O (pH 8.0 and 295 K), obtained under excitation through the ligand bands at 272 nm, display the typical $^5D_0 \rightarrow {}^7F_J$ (Eu^{III}, $J = 0-4$) or $^5D_4 \rightarrow {}^7F_J$ (Tb^{III}, $J = 6-3$) transitions (Figure 4). The excitation spectra recorded upon metal centered emission are very similar to the corresponding absorption spectra, indicating that the coordinated picolinate moieties provide an efficient energy transfer to the Eu^{III} and Tb^{III} ions. In addition to the typical $^5D_0 \rightarrow {}^7F_J$ transitions, the emission spectrum of the Eu^{III} complex shows a broad emission band with a maximum at about 387 nm. The intensity of this band quickly diminishes when a short delay (0.1 ms) is enforced and therefore has been attributed to the ligand centered $^1\pi\pi^*$ state. These results indicate that the bp12c4 ligand sensitizes more efficiently Tb^{III} than Eu^{III}, as often observed for Ln^{III} complexes with ligands bearing picolinate chromophores.[43]

Table 4. Luminescence Lifetimes of bp12c4 Complexes and Number of Inner-Sphere Water Molecules (q)

Ln	τ_{H2O} (τ_{D2O})/ms	equation[a]	q
Eu	0.52 (1.56)	$q_{Eu} = 1.05\Delta k_{obs}$[40]	1.36
		$q_{Eu} = 1.2(\Delta k_{obs} - 0.25)$[41]	1.25
		$q_{Eu} = 1.11(\Delta k_{obs} - 0.31)$[42]	1.09
Tb	1.48 (2.32)	$q_{Tb} = 4.2\Delta k_{obs}$[40]	1.03
		$q_{Tb} = 5.0(\Delta k_{obs} - 0.06)$[41]	0.92

[a] $\Delta k_{obs} = k_{obs}(H_2O) - k_{obs}(D_2O)$ and $k_{obs}=1/\tau_{obs}$.

The emission lifetimes of the $Eu(^5D_0)$ and $Tb(^5D_4)$ excited levels have been measured in D_2O and H_2O solutions of the complexes and were used to calculate the number of coordinated water molecules q. The results (Table 4) indicate the presence of at least one inner-sphere water molecule. The q values obtained for the Tb^{III} complex are close to one, and a general formula of $[Tb(bp12c4)(H_2O)]^+$ can be proposed for this complex in solution. However, the q values obtained in the case of the Eu^{III} analogue range between 1.09 and 1.36 depending on the particular equation used for the determination of the inner-sphere water molecules. These results suggest a change in hydration number from $q = 2$ to $q = 1$ occurring close to the middle of the lanthanide series. The hydration state was further assessed by a variable-temperature UV−vis study on an aqueous solution of the Eu^{III} analogue. Indeed, it has been previously demonstrated that the $^5D_0 \leftarrow {}^7F_0$ transition band of Eu^{III} is very sensitive to the coordination environment and can be used to test the presence of differently hydrated species.[44,45] In the region of the $^5D_0 \leftarrow {}^7F_0$ transition, the spectrum of the $[Eu(bp12c4)(H_2O)_q]^+$ complex shows two absorption bands at 579.4 and 579.9 nm, with an intensity ratio that changes with temperature: the band at shorter wavelengths is decreasing, while that at longer wavelengths is increasing with temperature (see Supporting Information). Analogously to previously reported systems, we related this temperature dependency to an hydration equilibrium. On the basis of the q values obtained from the luminescence lifetime data ($1 < q < 2$), we expect that this equilibrium exists between a monohydrated and a dihydrated complex:

$$[Eu(bp12c4)(H_2O)_2]^+ \leftrightarrow [Eu(bp12c4)(H_2O)]^+ + H_2O \quad (2)$$

The equilibrium constant corresponding to eq (2) may be written as

(37) Horrocks, W. D., Jr.; Sudnick, D. R. *Acc. Chem. Res.* **1981**, *14*, 384–392.
(38) Dickins, R. S.; Aime, S.; Batsanov, A. S.; Beeby, A.; Botta, M.; Bruce, J. I.; Howard, J. A. K.; Love, C. S.; Parker, D.; Peacock, R. D.; Puschmann, H. *J. Am. Chem. Soc.* **2002**, *124*, 12697–12705.
(39) Renaud, F.; Piguet, C.; Bernardelli, G.; Bünzli, J-C. G.; Hopfgartner, G. *Chem.—Eur. J.* **1997**, *3*, 1646–1659.
(40) Horrocks, W. D., Jr.; Sudnick, D. R. *J. Am. Chem. Soc.* **1979**, *101*, 334–340.
(41) Beeby, A.; Clarkson, I. M.; Dickins, R. S.; Faulkner, S.; Parker, D.; Royle, L.; de Sousa, A. S.; Williams, J. A. G.; Woods, M. *J. Chem. Soc., Perkin Trans. 2* **1999**, 493–504.
(42) Supkowski, R. M.; Horrocks, W. D., Jr. *Inorg. Chim. Acta* **2002**, *340*, 44–48.
(43) Nonat, A.; Gateau, C.; Fries, P. H.; Mazzanti, M. *Chem.—Eur. J.* **2006**, *12*, 7133–7150.
(44) Graeppi, N.; Powell, D. H.; Laurenczy, G.; Zékány, L.; Merbach, A. E. *Inorg. Chim. Acta* **1995**, *235*, 311–326.
(45) Platas-Iglesias, C.; Corsi, D. M.; Vander Elst, L.; Muller, R. N.; Imbert, D.; Bünzli, J-C. G.; Tóth, É.; Maschmeyer, T.; Peters, J. A. *J. Chem. Soc., Dalton Trans.* **2003**, 727–737.

$$K_{Eu} = \frac{[[Eu(bp12c4)(H_2O)]^+]}{[[Eu(bp12c4)(H_2O)_2]^+]} \quad (3)$$

The reaction enthalphy, $\Delta H°$, and the reaction entropy, $\Delta S°$, for the equilibrium are obtained from the temperature dependence of K_{Eu}

$$\ln K_{Eu} = \frac{\Delta S°}{R} - \frac{\Delta H°}{RT} \quad (4)$$

The temperature dependent equilibrium constants for the hydration equilibrium 2 have been determined as previously described.[44] The temperature dependence of the relative intensities of the two bands in the absorption spectra was used to determine the reaction enthalpy, $\Delta H° = 9.5 \pm 0.6$ kJ mol^{-1}, and the reaction entropy, $\Delta S° = 33 \pm 2$ J mol^{-1} K^{-1} (Supporting Information). A q value of 1.4 is calculated at 298 K which is in fairly good agreement with that obtained from luminescence measurements for the Eu^{III} complex. This agreement appears to confirm that it is indeed correct to analyze the UV−vis spectra by assuming similar oscillator strengths for the two $^5D_0 \leftarrow ^7F_0$ transitions.[5]

Conformational Analysis. To obtain information on the solution structure of the Ln^{III} complexes of bp12c4 we have characterized these systems by means of DFT calculations (B3LYP model). Because the experimental data indicate a change in the hydration number from $q = 2$ to $q = 1$ around the middle of the lanthanide series, we have investigated the $[Ln(bp12c4)(H_2O)]^+$ (Ln = Gd, Ho, Yb, or Lu) and $[Ln(bp12c4)(H_2O)_2]^+$ (Ln = La, Nd, Gd) systems. The effective core potential (ECP) of Dolg et al. and the related [5s4p3d]-GTO valence basis set were applied in these calculations. This ECP includes 46 + 4f^n electrons in the core, leaving the outermost 11 electrons to be treated explicitly, and it has been demonstrated to provide reliable results for several lanthanide complexes with both macrocyclic[46,47] or acyclic[48] ligands. Compared to all-electron basis sets, ECPs account to some extent for relativistic effects, which are believed to become important for the elements from the fourth row of the periodic table. The NMR spectra of the diamagnetic La^{III} and Lu^{III} complexes indicate that the complexes adopt a rigid C_2 symmetry in solution. There are eight possible conformations of the complexes of bp12c4 (four enatiomeric pairs of diasteroisomers) consistent with a C_2 symmetry (Chart 1). In fact, the complexes of bp12c4 present two sources of helicity: one associated with the layout of the picolinate pendant arms (absolute configuration Δ or Λ) and the other to the four five-membered chelate rings formed by the binding of the crown moiety (each of them showing absolute configuration δ or λ). Because enantiomers have the same physicochemical properties in a nonchiral environment, we have only considered four diasteroisomeric forms of the complexes in our conformational analysis:

Chart 1. (Top) Four Possible Enantiomeric Pairs of Diasteroisomers for Ln^{III}bp12c4 Complexes within the C_2 Point Group[a] and (Bottom) Sources of Chirality Due to the Layout of the Pendant Arms (Λ or Δ) and the Conformation of the Crown Moiety (λ or δ)

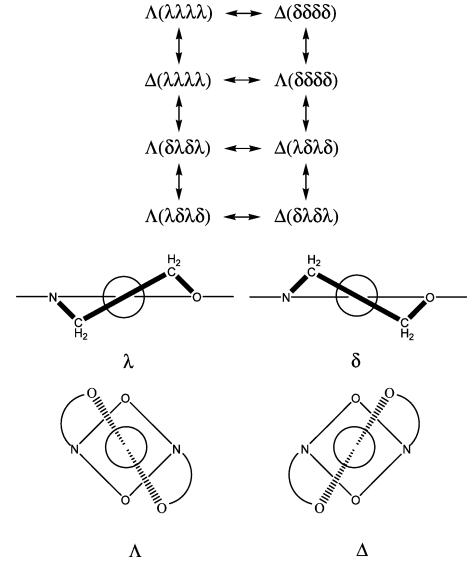

[a] Vertical arrows relate diastereoisomeric forms, while the horizontal ones relate enantiomeric pairs.

$\Lambda(\lambda\lambda\lambda\lambda)$, $\Delta(\lambda\lambda\lambda\lambda)$, $\Lambda(\delta\lambda\delta\lambda)$, and $\Lambda(\lambda\delta\lambda\delta)$. Optimized Cartesian coordinates for the different $[Ln(bp12c4)(H_2O)_q]^+$ complexes (q = 1 or 2) are given in the Supporting Information.

In the case of the $[Ln(bp12c4)(H_2O)]^+$ complexes (Ln = Gd, Ho, Yb, or Lu), our geometry optimizations performed in vacuo provide three minimum energy conformations of the complexes: $\Lambda(\lambda\lambda\lambda\lambda)$, $\Delta(\lambda\lambda\lambda\lambda)$, and $\Lambda(\delta\lambda\delta\lambda)$. All calculated structures for all conformations show nearly undistorted C_2 symmetries. Any attempt to model the $\Lambda(\lambda\delta\lambda\delta)$ form of the complexes systematically led to conformations $\Lambda(\lambda\lambda\lambda\lambda)$ or $\Delta(\lambda\lambda\lambda\lambda)$ during the geometry optimization process, indicating that the $\Lambda(\lambda\delta\lambda\delta)$ form is not a local minimum on the potential energy surface. It is also noteworthy that in the optimized geometries of the Yb^{III} and Lu^{III} complexes showing $\Lambda(\lambda\lambda\lambda\lambda)$ conformation the water molecule is hydrogen bonded to one of the carboxylate groups rather than coordinated to the lanthanide ion.

The relative free energies of the $\Lambda(\lambda\lambda\lambda\lambda)$ and $\Lambda(\delta\lambda\delta\lambda)$ conformations of q = 1 complexes with respect to the $\Delta(\lambda\lambda\lambda\lambda)$ one were calculated in aqueous solution from solvated single point energy calculations (C-PCM model) on the geometries optimized in vacuo. Relative free energies were calculated as $\Delta G^{sol} = G^{sol}_X - G^{sol}_{\Delta(\lambda\lambda\lambda\lambda)}$ and therefore a positive relative energy indicates that the $\Delta(\lambda\lambda\lambda\lambda)$ conformation is more stable than the X one. According to our DFT calculations the $\Lambda(\delta\lambda\delta\lambda)$ conformation is the most stable one for all the lanthanides investigated. However, the energy difference between the $\Lambda(\delta\lambda\delta\lambda)$ and $\Delta(\lambda\lambda\lambda\lambda)$ conformations is relatively small, especially for the heaviest lanthanide ions. In the solid state the Gd^{III} complex crystallizes as the two centrosymmetrically related enantiomers $\Lambda(\lambda\lambda\lambda\delta)$ and $\Delta(\delta\delta\delta\lambda)$. To evaluate the relative stability of the conformation observed in the solid state with respect to

(46) Gonzalez-Lorenzo, M.; Platas-Iglesias, C.; Avecilla, F.; Faulkner, S.; Pope, S. J. A.; de Blas, A.; Rodriguez-Blas, T. *Inorg. Chem.* **2005**, *44*, 4254–4262.
(47) Cosentino, U.; Villa, A.; Pitea, D.; Moro, G.; Barone, V.; Maiocchi, A. *J. Am. Chem. Soc.* **2002**, *124*, 4901–4909.
(48) Quali, N.; Bocquet, B.; Rigault, S.; Morgantini, P.-Y.; Weber, J.; Piguet, C. *Inorg. Chem.* **2002**, *41*, 1436–1445.

Table 5. Relative Free Energies in Aqueous Solution (C-PCM, B3LYP/6-31G(d)) of the $\Lambda(\lambda\lambda\lambda\lambda)$ and $\Lambda(\delta\lambda\delta\lambda)$ Isomers with Respect to the $\Delta(\lambda\lambda\lambda\lambda)$ One in $[Ln(bp12c4)(H_2O)_q]^+$ Complexes ($q = 1$ or 2)[a]

	$[Ln(bp12c4)(H_2O)]^+$		$[Ln(bp12c4)(H_2O)_2]^+$	
	$\Lambda(\lambda\lambda\lambda\lambda)$	$\Lambda(\delta\lambda\delta\lambda)$	$\Lambda(\lambda\lambda\lambda\lambda)$	$\Lambda(\delta\lambda\delta\lambda)$
La			*b*	2.74
Nd			*b*	3.21
Gd	5.80	−1.07	*b*	*b*
Ho	6.27	−0.58		
Yb	*b*	−0.45		
Lu	*b*	−0.28		

[a] $\Delta G^{sol} = G^{sol}_X - G^{sol}_{\Delta(\lambda\lambda\lambda\lambda)}$ and therefore a positive relative energy indicates that the $\Delta(\lambda\lambda\lambda\lambda)$ conformation is more stable than the X one. Values in kcal mol^{-1}. [b] A water molecule leaves the inner-sphere coordination environment during the geometry optimization process.

the $\Delta(\lambda\lambda\lambda\lambda)$ one we have performed a geometry optimization of the $[Gd(bp12c4)(H_2O)_q]^+$ system by using the X-ray crystal structure of this complex as input geometry. In this calculation the oxygen atom of a neighboring $[Gd(bp12c4)]^+$ unit coordinated to the metal ion was replaced by an inner sphere water molecule. The subsequent solvated single point energy calculation on the geometry optimized in vacuo indicates that the $\Lambda(\lambda\lambda\lambda\delta)$ conformation observed in the solid state is less stable than the $\Delta(\lambda\lambda\lambda\lambda)$ one by 1.23 kcal·mol^{-1} (2.30 kcal·mol^{-1} with respect to the $\Lambda(\delta\lambda\delta\lambda)$ form). This result is consistent with the C_2 symmetry of the complexes in solution indicated by the NMR spectra.

For $[Ln(bp12c4)(H_2O)_2]^+$ complexes (Ln = La, Nd, or Gd), our geometry optimizations provide the two minimum energy conformations, $\Lambda(\delta\lambda\delta\lambda)$ and $\Delta(\lambda\lambda\lambda\lambda)$, while geometry optimizations of the $\Lambda(\lambda\lambda\lambda\lambda)$ conformation gave $q = 1$ structures for all the lanthanides investigated. A similar situation was also observed for the $\Lambda(\delta\lambda\delta\lambda)$ conformation in the case of the Gd complex. These results suggest that the $\Delta(\lambda\lambda\lambda\lambda)$ conformation is the most favorable one for the coordination of two water molecules. The relative energies of the $\Lambda(\delta\lambda\delta\lambda)$ and $\Delta(\lambda\lambda\lambda\lambda)$ conformations in aqueous solution indeed show that the later one is more stable than the first by about 3 kcal·mol^{-1} (Table 5).

The minimum energy conformations calculated for the $[Gd(bp12c4)(H_2O)_q]^+$ complexes ($q = 1$ or 2) are shown in Figure 5 while selected bond distances and angles of the metal coordination environments are given in Table 6. As expected, the bond distances of the metal coordination environments are in general longer for the $q = 2$ complex than for the $q = 1$ one. The $Gd-O_W$ distance calculated for the $[Gd(bp12c4)(H_2O)]^+$ system (2.585 Å) is slightly longer than that normally assumed in the analysis of ^{17}O NMR longitudinal relaxation data of nine-coordinate Gd^{III} complexes (2.50 Å). However, this is expected because our DFT calculations were performed in vacuo. In aqueous solution the $Ln-O_W$ bond distances get shorter because of a stronger water-ion interaction arising from solvent polarization effects that, increasing the dipole moment of the free water molecules, increase the water-ion interaction.[49] The angle described by the nitrogen atom of one pyridine unit, the lanthanide, and the nitrogen atom of the pyridine group of

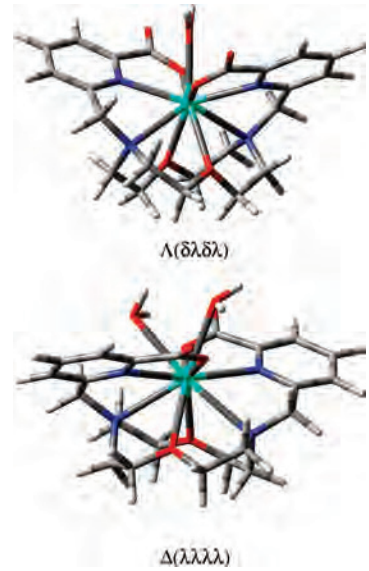

Figure 5. Calculated minimum energy conformations of the $[Gd(bp12c4)(H_2O)_q]^+$ complexes ($q = 1$ or 2) as optimized in vacuo at the B3LYP/6−31G(d) level.

Table 6. Values of the Main Geometrical Parameters of the Minimum Energy Conformations Calculated for $[Gd(bp12c4)(H_2O)_q]^+$ Complexes ($q = 1$ or 2) at the B3LYP/6-31G(d) Level[a]

	$q = 1$, $\Lambda(\delta\lambda\delta\lambda)$	$q = 2$, $\Delta(\lambda\lambda\lambda\lambda)$
$Gd-N_{PY}$	2.508	2.606(0.040)
$Gd-O_C$	2.608	2.602(0.082)
$Gd-O_{COO}$	2.317	2.370(0.019)
$Gd-O_W$	2.585	2.666(0.041)
$Gd-N_{AM}$	2.667	2.765
$N_{PY}-Gd-N_{PY}$	148.17	164.70
$O_{COO}-Gd-O_{COO}$	136.86	138.42
O_C-Gd-O_C	67.72	69.80
$N_{AM}-Gd-N_{AM}$	119.80	109.99

[a] Distances (Å), angles (deg.) with standard deviations within parenthesis. N_{AM} = amine nitrogen atoms; N_{PY} = pyridyl nitrogen atoms; O_{COO} = carboxylate oxygen atoms; O_C = crown oxygen atoms; O_W = water oxygen atoms.

the second pendant arms amounts to 164.7° for the $q = 2$ complex and 148.2° for the $q = 1$ one. These results suggest that the $\Delta(\lambda\lambda\lambda\lambda)$ conformation provides a more open structure that generates less steric hindrance for the two inner-sphere water molecules placed in between the two pendant arms. As a consequence, the most stable conformation for $q = 2$ complexes is the $\Delta(\lambda\lambda\lambda\lambda)$ while the minimum energy conformation for $q = 1$ complexes is the $\Lambda(\delta\lambda\delta\lambda)$ one.

Yb^{III}-Induced Paramagnetic Shifts. The binding of a ligand to a paramagnetic Ln^{III} ion generally results in large NMR frequency shifts at the ligand nuclei, with magnitudes and signs depending on both the nature of the lanthanide ion and the location of the nucleus relative to the metal center.[50] Thus, the analysis of the NMR spectra of Ln^{III} paramagnetic complexes can provide useful structural information in solution. For a given nucleus *i*, the isotropic paramagnetic shift induced by a lanthanide ion *j* (δ_{ij}^{para}) is generally a combination of the Fermi contact (δ_{ij}^{con}) and the dipolar (δ_{ij}^{dip}) contributions:[50]

$$\delta_{ij}^{para} = \delta_{ij}^{exp} - \delta_i^{dia} = \delta_{ij}^{con} + \delta_{ij}^{dip} \quad (5)$$

where the diamagnetic contribution δ_i^{dia} is obtained by measuring the chemical shifts for analogous diamagnetic

(49) Djanashvili, K.; Platas-Iglesias, C.; Peters, J. A. *Dalton Trans.* **2008**, 602–607.

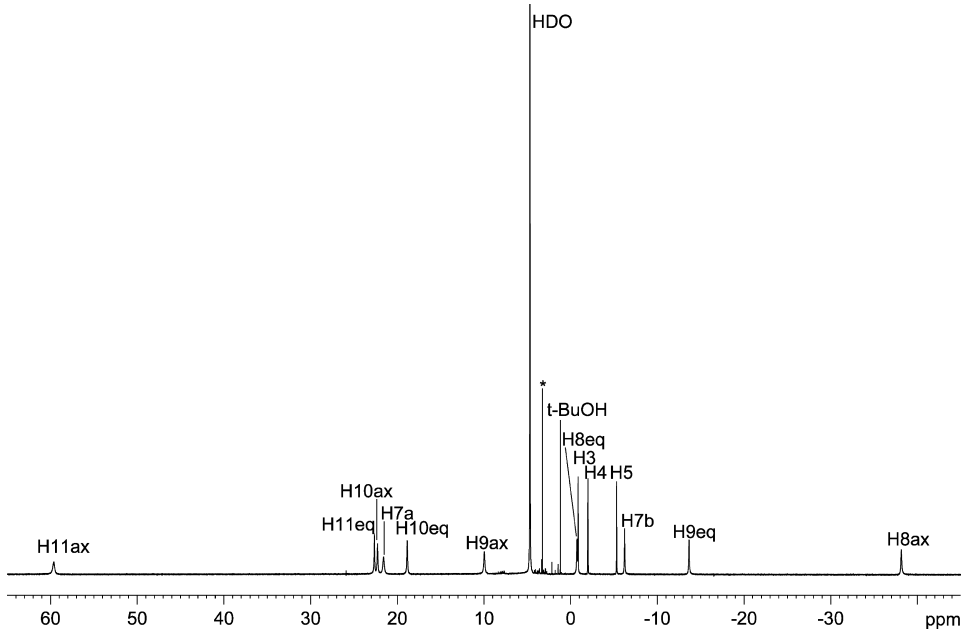

Figure 6. ^{1}H NMR spectrum (300 MHz) of $[Yb(bp12c4)(H_2O)]^+$ recorded in D_2O solution at 298 K. The asterisk (*) denotes a diamagnetic impurity.

complexes (the Lu^{III} complex in the present case). The hyperfine ^{1}H NMR shifts in Yb^{III} complexes are considered to be largely pseudocontact in origin, and we therefore initiated the analysis of the paramagnetic shifts observed in the ^{1}H NMR spectrum of the Yb^{III} complex with the assumption that they are dominated by dipolar contributions, as given by the following equation:

$$\delta_{ij}^{\mathrm{dip}} = D_1 \frac{3\cos^2\theta - 1}{r^3} + D_2 \frac{\sin^2\theta \cos 2\varphi}{r^3} \qquad (6)$$

where r, θ and φ are the spherical coordinates of the observed nucleus with respect to Ln^{III} at the origin and D_1 and D_2 are proportional, respectively, to the axial $[\chi_{zz} - 1/3(\chi_{xx} + \chi_{yy} + \chi_{zz})]$ and rhombic $(\chi_{xx} - \chi_{yy})$ anisotropies of the magnetic susceptibility tensor χ. In the special case of axial symmetry, the second term of eq 6 vanishes since $D_2 = 0$.

The ^{1}H NMR spectra of the paramagnetic complexes of the lightest Ln^{III} ions (Ce−Eu) show broad signals for many proton nuclei, presumably because of the presence of a hydration equilibrium in aqueous solution between $q = 1$ and $q = 2$ complexes. Our DFT calculations described above indicate that the hydration equilibrium is accompanied by a ligand conformational change. A significant energy barrier for this conformational change appears to be responsible for the exchange broadening observed in the NMR spectra of the complexes with the large Ln^{III} ions. However, the slow-exchange region for this process could not be reached even upon cooling a solution of the Eu^{III} complex at 278 K. Thus, the analysis of the paramagnetic shifts induced by the light Ln^{III} ions (Ce−Eu) was not possible.

The ^{1}H NMR spectrum of $[Yb(bp12c4)(H_2O)]^+$ (Figure 6) is well resolved and consists of 13 signals corresponding to the 13 different proton magnetic environments of the ligand (see Scheme 1 for labeling). This points to an effective C_2 symmetry of the complex in solution, as also observed for the diamagnetic La^{III} and Lu^{III} analogues. The assignments of the proton signals (Table 7) were based on standard 2D homonuclear COSY experiments, which gave strong cross-peaks between the geminal CH_2 protons (7−11) and between the ortho-coupled pyridyl protons. Additional cross-peaks between protons 8−9 and 10−11 allowed identifying the proton signals corresponding to each of the $N-CH_2-CH_2-O$ units. The ten ^{1}H NMR peaks due to protons 7−11 can be grouped into two different sets according to their relative line broadening: five resonances with linewidths at half-height of 40−84 Hz (at 300 MHz and 298 K) and five signals with linewidths in the range of 25−36 Hz (Figure 6). These two sets of signals correspond to two sets of Yb^{III}−proton distances, the broader resonances being associated with the

Table 7. ^{1}H Shifts (ppm with Respect to TMS) for the Yb^{III} Complex of bp12c4 and Comparison of Experimental and Calculated Dipolar ^{1}H Shifts (ppm)

	δ_i^{exp}	δ_i^{para}[a]	δ_i^{dip}[b]	δ_i^{dip}[b,c]
H3	−0.85	8.88	9.76	9.92
H4	−1.99	10.23	10.77	10.85
H5	−5.30	13.13	13.93	14.06
H7a	21.57	−17.14	−18.23	−17.25
H7b	−6.21	10.98	8.45	8.77
H8ax	−38.14	41.32	40.91	40.93
H8eq	−0.73	4.27	6.68	6.27
H9ax	9.97	−6.58	−7.23	−8.77
H9eq	−13.65	17.44	5.88	*c*
H10ax	22.27	−18.09	−15.17	−16.15
H10eq	18.86	−14.52	−16.19	−16.24
H11ax	59.63	−56.72	−58.38	−57.00
H11eq	22.64	−19.04	−16.68	−16.63
AF_j			0.1558	0.0659
D_1			−372 ± 67	−426 ± 30
D_2			2780 ± 80	2763 ± 35

[a] Positive values correspond to shifts to higher fields. The diamagnetic contribution was estimated from the shifts observed for the Lu^{III} analogue. [b] Values calculated by using eq 3 and the B3LYP/6−31G(d) optimized structure of $[Yb(bp12c4)(H_2O)]^+$ with $\Lambda(\delta\lambda\delta\lambda)$ conformation. [c] H9eq was excluded from the fitting procedure (see text).

(50) Peters, J. A.; Huskens, J.; Raber, D. J. *Prog. NMR Spectrosc.* **1996**, *28*, 283–350.

protons closer to the metal ion.[51] Thus, the broader resonances were assigned to axial protons, while the second set of signals was assigned to equatorial ones. A careful examination of the Yb···H distances in the different DFT optimized structures calculated for the $[Yb(bp12c4)(H_2O)]^+$ system shows that the H11ax protons present a particularly short Yb···H distance. This is in agreement with the line-broadening data which show a line width at half-height of 84.4 Hz for the signal at 59.63 ppm, while appreciably sharper peaks are observed for the remaining axial protons of the crown moiety [40−63 Hz]. On this basis, the signal at 59.63 ppm was assigned to the H11ax protons, and subsequently a full assignment of the spectrum was achieved (Table 7).

The analysis of the paramagnetic shifts to get structural information is generally initiated by assuming a certain structure for the complex in solution, thereby allowing the calculation of the geometric factors. A common practice is to assume that the structure in solution is the same as that determined in the solid state by X-ray crystallography,[52] or an alternative approach is to use molecular[53,54] or quantum mechanical[55] calculations to approximate the structure of a complex. The calculated DFT geometries of $[Yb(bp12c4)(H_2O)]^+$ in $\Lambda(\lambda\lambda\lambda\lambda)$, $\Delta(\lambda\lambda\lambda\lambda)$, and $\Lambda(\delta\lambda\delta\lambda)$ conformations were used to assess the agreement between the experimental and predicted Yb^{III}-induced paramagnetic shifts with the SHIFT ANALYSIS program.[16] The SHIFT ANALYSIS program calculates the dipolar shifts defined by eq 6 in the molecular coordinate system by using a linear least-squares search that minimizes the difference between the experimental and calculated data. The agreement between the experimental and calculated isotropic shifts obtained by using the $[Yb(bp12c4)(H_2O)]^+$ calculated structures showing $\Lambda(\lambda\lambda\lambda\lambda)$ and $\Delta(\lambda\lambda\lambda\lambda)$ conformations is very poor (AF_j = 0.49 and 0.50, respectively). However, a much better agreement factor is obtained for the complex in the $\Lambda(\delta\lambda\delta\lambda)$ conformation [AF_j = 0.1558, eq 1]. Moreover, a dramatic improvement of the agreement factor is obtained when the H9eq protons are excluded from the fitting procedure [AF_j = 0.0657, Table 7]. Similar agreement factors were previously obtained for nonaxial Yb^{III} complexes according to the dipolar model.[56] The dramatic improvement of the agreement factor upon excluding protons H9eq from the fitting procedure may be related to (i) an important contact contribution for these nuclei and (ii) discrepancies between the structural model and the real structure of the complex in solution. Table 6 shows the D_1 and D_2 values providing the best fit of the experimental shift values, as well as a comparison of the experimental and calculated paramagnetic shifts according to the dipolar model.

The starting molecular axis system had the Yb^{III} ion at the origin, with the z axis containing the oxygen atom of the inner-sphere water molecule. Thus, the z axis is coincident with the C_2 symmetry axis of the molecule. The position of the x axis was chosen such that it forms an angle of 72.4° with the projection of the $Ln-O_{COO}$ vector on the xy plane (O_{COO} is the oxygen atom of the carboxylate group coordinated to the Yb^{III} ion). As expected for a nonaxial system, the χ susceptibility tensor obtained in the molecule fixed axis system is rhombic and was diagonalized, providing a set of Euler angles that relate the principal magnetic axis system to the molecular coordinate system. The best fitting parameters (excluding the H9eq protons) provide Euler angles with values close to zero, indicating that the magnetic axes are coincident with the molecular axes chosen for the system.

The analysis of the Yb^{III}-induced paramagnetic shifts unambiguously proves that this complex presents a $\Lambda(\delta\lambda\delta\lambda)$ conformation in aqueous solution, in agreement with the relative free energies reported in Table 5. Moreover, the data presented in Table 5 indicate a stabilization of this conformation when increasing the ionic radius of the lanthanide ion. Thus, the results obtained from DFT calculations in combination with the analysis of the Yb^{III}-induced paramagnetic shifts demonstrate that the $[Ln(bp12c4)(H_2O)]^+$ complexes adopt a $\Lambda(\delta\lambda\delta\lambda)$ conformation in aqueous solution across the lanthanide series from Gd to Yb.

Conclusions

In this work we have presented a new macrocyclic octadentate ligand designed for stable complexation of lanthanide ions. The hydration numbers obtained from luminescence lifetime measurements and UV−vis spectrophotometry indicate that an equilibrium in aqueous solution exists for Eu^{III} between a ten-coordinate species with two inner-sphere water molecules and a nine-coordinate complex with one inner-sphere water molecule. Theoretical calculations performed at the DFT (B3LYP) level evidence that the change in hydration number is accompanied by a change in the conformation that the complexes adopt in solution [$\Delta(\lambda\lambda\lambda\lambda)$ for $q = 2$ and $\Lambda(\delta\lambda\delta\lambda)$ for $q = 1$]. A significant energy barrier for this conformational change appears to be responsible for the exchange broadening observed in the NMR spectra of the complexes with the large Ln^{III} ions (Ln = La−Eu). The analysis of the Yb^{III}-induced paramagnetic shifts unambiguously indicates that this complex presents a $\Lambda(\delta\lambda\delta\lambda)$ conformation in aqueous solution, in agreement with the predictions of our DFT calculations. These results prove that DFT calculations combined with experimental information from NMR spectroscopy represent a powerful tool to obtain structural information of lanthanide complexes in solution. A careful examination of the solution structure is particularly important in complexes with relatively flexible ligands such as bp12c4, as the structure of the complexes in the solid state and in solution migh be substantially different

(51) Aime, S.; Barbero, L.; Botta, M.; Ermondi, G. *J. Chem. Soc., Dalton Trans.* **1992**, 225–228.
(52) Platas, C.; Avecilla, F.; de Blas, A.; Geraldes, C. F. G. C.; Rodríguez-Blas, T.; Adams, H.; Mahía, J. *Inorg. Chem.* **1999**, *38*, 3190–3199.
(53) Di Bari, L.; Pescitelli, G.; Sherry, A. D.; Woods, M. *Inorg. Chem.* **2005**, *44*, 8391–8398.
(54) Platas-Iglesias, C.; Piguet, C.; Andre, N.; Bünzli, J.-C. G. *J. Chem. Soc., Dalton Trans.* **2001**, 3084–3091.
(55) Fernández-Fernández, M. del C.; Bastida, R.; Macías, A.; Pérez-Lourido, P.; Platas-Iglesias, C.; Valencia, L. *Inorg. Chem.* **2006**, *45*, 4484–4496.
(56) Lisowski, J.; Sessler, J. L.; Lynch, V.; Mody, T. D. *J. Am. Chem. Soc.* **1995**, *117*, 2273–2285.

because crystal forces may favor a higher energy conformation in the solid.

Acknowledgment. M.M.-I., A.R.-S., D.E.-G., C.P.-I., A.de B., and T.R.-B. thank Ministerio de Educación y Ciencia and FEDER (CTQ2006-07875/PPQ) for financial support. This research was performed in the framework of the EU COST Action D38 "Metal-Based Systems for Molecular Imaging Applications". The authors are indebted to Centro de Computación de Galicia for providing the computer facilities.

Supporting Information Available: Optimized Cartesian coordinates (Å) of the complexes investigated in this work; UV−vis spectra of the Eu^{3+} complex. This material is available free of charge via the Internet at http://pubs.acs.org.

IC800878X